Desalination and Water Treatment
www.deswater.com

doi: 10.5004/dwt.2018.22378

121 (2018) 139–146
July

An EEMD and BP neural network hybrid approach for modeling regional sea level change

Lei He[a,b], Jilong Chen[c], Yue Zhang[b], Tengjiao Guo[b], Guosheng Li[b,*]

[a]*Key Laboratory of Poyang Lake Wetland and Watershed Research (Ministry of Education), Jiangxi Normal University, Nanchang, Jiangxi, China, Tel. +86079188120537; email: helei@jxnu.edu.cn*
[b]*Key Laboratory of Land Surface Pattern and Simulation, Institute of Geographical Sciences and Natural Resources Research, Chinese Academy of Sciences, Beijing, China, Tel. +8601064889008; emails: ligs@igsnrr.ac.cn (G. Li), zhangyue.13b@igsnrr.ac.cn (Y. Zhang), guotj.15b@igsnrr.ac.cn (T. Guo)*
[c]*Chongqing Institute of Green and Intelligent Technology, Chongqing, China, Tel. +8602365935878; email: cjl47168@163.com*

Received 25 February 2018; Accepted 10 April 2018

ABSTRACT

Sea level prediction is essential and complicated in the context of climate change. Conventional methods developed for the prediction are still considered insufficient due to the complexity of the nonstationary and nonlinear sea level change. To improve the modeling accuracy of the sea level, this paper proposed a methodology combining the ensemble empirical mode decomposition (EEMD) and the back propagation (BP) neural network for monthly mean sea level record modeling in South China Sea. The results show that the EEMD can extract the signals with physical meanings according to their unique frequencies. The inputs of the BP, defined by the preprocessing of the original time series, turn out to be smoother and more regular, influencing the modeling in a positive way. The good performance of the hybrid method, with higher correlation coefficient (R = 0.89) and lower root square mean error (RMSE = 28.16 mm) between the modeling and the observed data, suggests an improved accuracy on sea level modeling than using the BP directly (with R = 0.76 and RMSE = 36.74 mm). This hybrid method can be further applied to sea level modeling in another region. The results of the study also suggest that the preprocessing of the original time series such as smoothing and denoising is significantly improving the modeling.

Keywords: Regional variations; Sea level oscillations; Pearl River Delta

1. Introduction

Sea level is a significant indicator and the result of climate change, and sea level prediction is of great interests to the science and public [1]. While major efforts have been made to understand the change of sea level, which is complex by many factors, the predictability of the driving processes is limited [2,3]. The projection of sea level change largely depends on the methods being used and varies greatly from regions to regions [4]. Therefore, selecting a proper method for modeling site-specific sea level change is a challenging task and essential for accurately predicting the future sea level variability.

The conventional approach to predict the sea level has been to model and predict the contribution components: modeling the change of snow and ice melting and thermal expansion of the ocean surface under the condition of the temperature rise by the atmosphere – ocean coupled model [5,6]. Based on the clear driven factors and their interaction mechanism, the dynamic model would provide a range of

* Corresponding author.

Presented at the 3rd International Conference on Recent Advancements in Chemical, Environmental and Energy Engineering, 15–16 February, Chennai, India, 2018.

projection for sea level change at large scale such as global scale [7]. Nevertheless, large uncertainties occur while applying this global model to regional sea level which is mainly affected by many local factors, and the physical process and mechanisms is difficult to be stimulated [8]. Rahmstorf [9] proposed a semi-empirical approach for sea level prediction by connecting the global sea level rise to global mean surface temperature. This method provides a pragmatic alternative for the global sea level prediction while the driver (e.g., global warming) is known but the computation of the link between the driver and the sea level response remains elusive. Furthermore, similar to the model prediction, the semi-empirical approach is not able to fully model the change for sea level in regional or along coasts where the drivers and their contributions are complex and uncertain. Another approach is to simulate the observed sea level time series and predict it by using mathematical statistics model. Nerem et al. [10] made extrapolation of the quadratic implies global mean sea level could rise 65 ± 12 cm by the year 2100 compared with the year 2005 [10]. As the model depends on the past and present observed records and the developed mathematical basis, this approach can simulate the sea level change well and is reliable for local long-term (e.g., decade) sea level prediction.

To improve the accuracy of the prediction, time series are often decomposed and analyzed as an ensemble of several simpler signals, such as cyclic components (e.g., seasonal, semi-annual and annual cycles), trends and random noise [11]. Huang et al. [12] proposed a new spectral decomposition algorithm for the analysis called empirical mode decomposition (EMD), which has been widely applied in sea level study [13,14]. The original time series are decomposed into several oscillating modes and a residual (trend), called intrinsic mode functions (IMFs) [15]. Unlike wavelet or Fourier analysis, EMD is a non-parametric method which does not require the use of pre-determined basis functions, and performs better while employed to the analysis of nonstationary series. A noise assisted method ensemble EMD (EEMD) was developed by Wu and Huang [16] as the improvement of EMD to address the mode mixing, a phenomenon that the similar frequencies mix with each other. These methods can lead to optimal improvements in the analyzing of the past and present time series, whereas they are limited in the prediction of future change.

On the other hand, approaches for modeling and predicting some geophysical time series have been well developed to enhance the ability of capturing the nonlinear or nonstationary characteristics (e.g., auto-regressive and moving average model [17], support vector machine [18], grey model [19]). Among these methods, artificial neural network (ANN) has been widely used in various areas for the prediction of nonlinear and nonstationary time series with its highly learning function [20]. Back propagation (BP) algorithm has been the most representative and developed method for ANN and applied to model the sea level and tidal changes [21]. However, as a pure data-driven model, none of any physical relationships can be pre-determined from the time series by using BP neural network, thus the prediction finally provides several dataset without any physical meaning patterns can be explored or explained. Establishment of a scientific method to extract the distinctive temporal patterns of sea level variations and investigation of the major factors is essential for improving the modeling and prediction accuracy of the regional sea level.

Guangdong Province, one of the most essential financial centers in China, is located in southern China and abuts the northern coast of the Pacific. Similar to other coastal regions in the world, the threat posed by rising sea level has become more prominent in Guangdong due to the low-lying nature of the land, the increasing population and assets, and the effects of climate change [22]. Many studies have been conducted to predict sea level change in Guangdong at both large and small scales, whereas no agreement has been reached [23]. Accurate prediction of the regional sea level variations in Guangdong has been impeded by the complex forcing factors and the relatively short-term coverage provided by satellite altimetry data [24].

To address this, this study attempts to propose a hybrid method combining EEMD and BP neural network (EEMD-BP) to model the sea level change from the long term monthly tide gauge records (spanning 01/1959–12/2011) on the coast of Guangdong. EEMD is used to pre-process the original time series, in other words, to analyze the patterns of regional sea level change, figure out the main affecting factors, and in turn make the original time series simpler. BP neural network is then applied to predict the patterns, and the result of modeling the original time series is obtained by reconstructing the output of the prediction. This method explores the ways of improving the prediction accuracy at regional scale and may provide potential for investigation of the patterns of sea level change.

2. Data and methods

The method of EEMD-BP involves two parts: the decomposition of the original time series and the signals prediction. At first the original sea level time series is decomposed by using EEMD for smoothing and denoising, and several simpler signals (such as cyclic components, trends and random) called IMFs, are obtained. Then prediction models are established for modeling the variability of each IMF by using BP neural network. Finally the future change of the original sea level time series is simulated by reconstructing the output of each IMF from the prediction models.

2.1. Ensemble empirical mode decomposition

EMD extracts the frequency contributions, that is, IMFs, from a targeted time series oscillatory signal. An IMF usually has a physical meaning and can be identified by two characteristics: (1) the number of extremes and zero-crossings are either equal or differ at most by one; (2) at any point, the mean value defined by local envelops of the IMF must be zero.

The detailed procedures of EMD are described as follows [25]: First of all, local maxima and minima are identified in a signal $f(t)$, then an upper envelope and a lower envelope are produced by employing cubic interpolation functions, respectively. Second, the local mean $m_1(t)$, defined as half the difference between the upper and lower envelopes, is computed and subtracted from $f(t)$. Usually the residual signal $h_1(t)$ is not stable and above procedure is repeated until the criteria of IMF is satisfied. Then the first IMF $IMF_1(t)$, that

is, the highest frequency component in $f(t)$, can be extracted after several times (e.g., k times) of sifting process:

$$\mathrm{IMF}_1(t) = h_{1k}(t) = h_{1(k-1)}(t) - m_{1(k)}(t) \quad (1)$$

Now $f(t)$ has been decomposed into the highest frequency component, $\mathrm{IMF}_1(t)$, and a residual signal, as in the following equation

$$f(t) = \mathrm{IMF}_1(t) + R_1(t) \quad (2)$$

Iterate on the residual until the stop criteria is met and the process of the sifting is complete. Finally, the original signal has been decomposed into several IMFs (e.g., after n times decomposition, there are n IMFs) and the final residual, or trend, as show in the following equation:

$$f(t) = \sum_{j=1}^{n} \mathrm{IMF}_j(t) + R_n(t) \quad (3)$$

However, mode mixing often came out as the result of signal intermittence and noise. Therefore, EEMD was proposed to eliminate the effect of mode mixing and extract the actual time–frequency distribution of the signal by Wu and Huang [26]. The original signal is added to an ensemble of white noise which is uniformly distributed as white background, and the bits of signals of different scales can be automatically designed onto proper scales of reference established by the white noise. Each individual trial produces very noisy results, consisting of real signal and noise. The noise can be averaged out as more and more trials are added in the ensemble, and the only persistent part is the signal.

Two parameters, the number of white noise series M and amplitude of the added noise ε, affect the decomposing results of the EEMD, which is evaluated by the final standard deviation of error e (the distinctions between the input time series and the corresponding IMFs),

$$e = \frac{\varepsilon}{\sqrt{M}} \quad (4)$$

In general, the M of a few hundred will gain a good result, and the remaining noise may cause only less than 1% of error. In addition, under an appropriate level of the ε, it has no obvious improvement for decomposing results by constantly increasing the M. Based on these findings above, meaningful IMFs can be well specified when M = 100, and ε ∈ [0.01, 0.5] [16]. In this study, the number of ensemble white noise is 100, and the ratio of the standard deviation of the white noise and that of the original signal was 0.2.

2.2. BP neural network

BP neural network is the most prevalent learning algorithm in ANNs due to its excellent properties such as the universal approximating ability toward arbitrary continuous functions [27]. The principle of BP neural network is based on the hypothesis that there is a functional relationship between the observation and the prediction, and the prediction is approached by means of establishing the neural network to simulate the relationship. Fig. 1 shows the typical BP neural

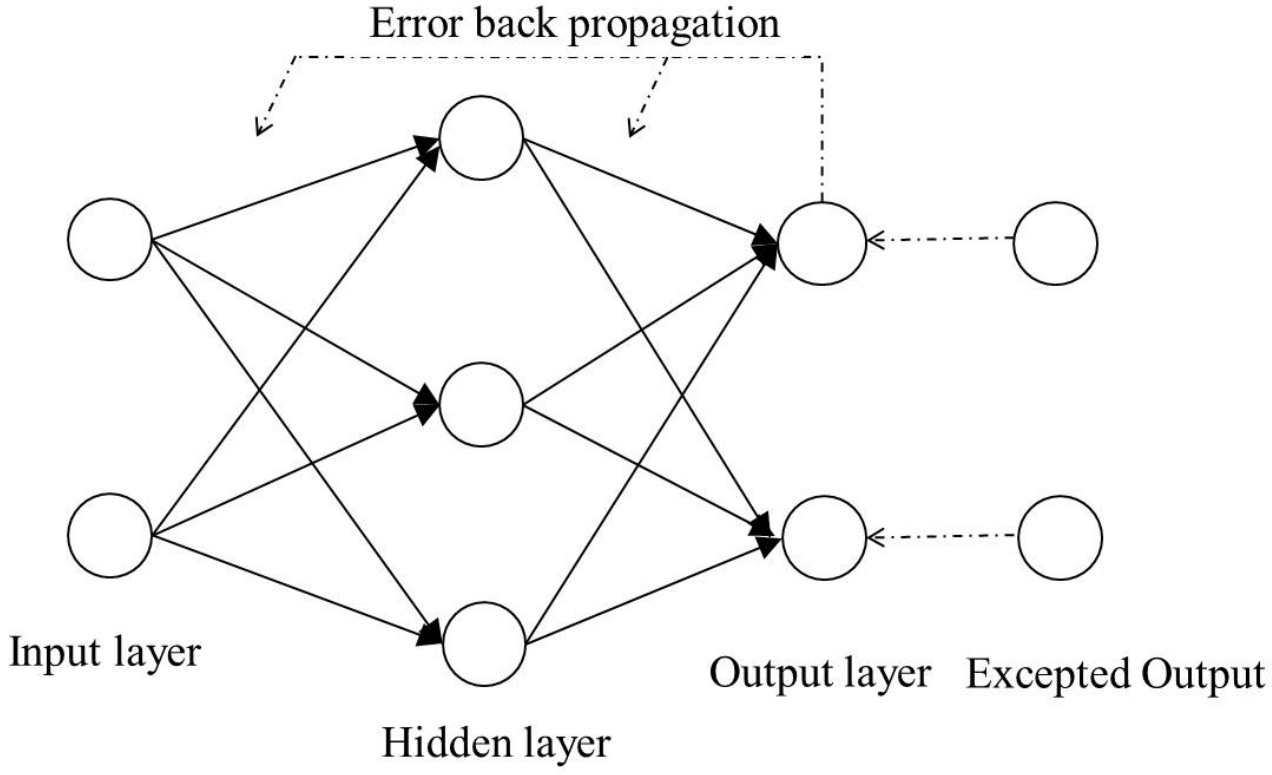

Fig. 1. Structure of BP neural network.

network structure which has three layers: input layer, hidden layer and output layer, and each layer consists of several neurons and all the layers are interconnected by sets of correlation weights. The modeling procedure includes two parts: forward information transmission and the error BP. At the first stage, the input signals flow from the input layer to the hidden layer, and transform to the output layer and then the outputs are produced by means of a non-linear transfer function. A common transformation is the tan-sigmoid function expressed by $f(x) = 2/(1 + \exp(-2 \times x)) - 1$, which produces the output between –1 and 1. The output may be very different from the required data, since all the weights are random at first. Therefore, the error BP procedure starts. Each error of the neuron is calculated and minimized through gradient descent while propagating to the prior layers. The weights are modified on the repeated processes of information transmission and error propagation until the error can be accept or the preset training time is reached, then the network is established. Since the principle of BP neural network has been developed and described by many studies in details [20], in this paper a brief introduction is given.

2.3. Assessment of model performance

To enlighten the improvements of the hybrid method, two predictions are carried out and compared by using the BP neural network and EEMD-BP, respectively. Prediction with BP method is to simulate the original sea level time series directly by BP neural network, without any preprocessing process such as decomposing and denoising.

To assess the performances of the models, correlation coefficient (R) and root mean square error (RMSE) are determined. RMSE provides information on the short-term performance of the correlations by allowing a term by term comparison of the actual deviation between the observed and predicted values. RMSE is calculated by the following equations.

$$\mathrm{RMSE} = \sqrt{\frac{1}{n}\sum_{i=1}^{n}(y_i - \hat{y}_i)^2} \tag{5}$$

where n, y, $\hat{y}$ represent the number of samples, the observed value and the prediction, respectively.

2.4. Data and model development

Zhapo tide gauge, which is located in the southern China (21°35′N, 111°50′E), provides the longest and most complete records widely used for the estimation of sea level change in the South China Sea. Therefore, the monthly series of Zhapo tide gauge during the period 01/1959–12/2011 selected from Permanent Service for Mean Sea Level (PSMSL) were used here to illustrate the capability of the proposed model for sea level prediction. Small gaps in the records (1–2 months) were filled using cubic spine interpolation [28].

One of the difficulties in establishing the BP neural network model for sea level prediction is to construct the input datasets. To overcome the sparse of the samples, more time series are created by moving a window on the original IMFs. For learning and predicting the rules precisely, at least one complete cycle should be contained in the window. Given that the nutation cycle, with the period of 18.61 years, is a relatively long observed cycle in sea level change, after some tests, a window including 360 samples (i.e., covering 30 years) are established to create the new input datasets. Hence, the original time series spanning 01/1959–12/2011 (containing 636 samples) are reconstructed to 288 groups of data. And these 288 groups are then separated into two parts for modeling, the first 228 groups are training datasets and the last 60 are validation datasets. For example, the input layer contains 30 samples, which are January records from 1959 to 1988, and the output is the January record in 1989; then it moves to the next round and this input layer contains 30 February records from 1959 to 1988, and the corresponding output value is the February record of 1989. This process is moving on monthly until the input of December records spanning 1976–2005 and the output of December in 2006 are complete. Then the network with 30 neurons in the input layers and 1 neuron in output layer finishes training.

3. Results

The results first show the oscillations and long-term trend as obtained from the EEMD; then, the significance test of the oscillations is conducted and their physical meanings are discussed, and finally, the performance of the BP neural network is evaluated.

3.1. Decomposition of tide gauge records

The series of Zhapo tide gauge were decomposed into nine IMFs by EEMD, as shown in Fig. 2. The mean periods of IMFs 1–8 are 3, 7, 13, 26, 49, 121, 220 and 314 months, respectively, and the remainder IMF 9 is the long-term trend. To ensure the decomposition results are meaningful and not the noises, the significance test is conducted [29], as shown in Fig. 3. IMFs 1–3 and IMFs 5–7 pass the significance test on the

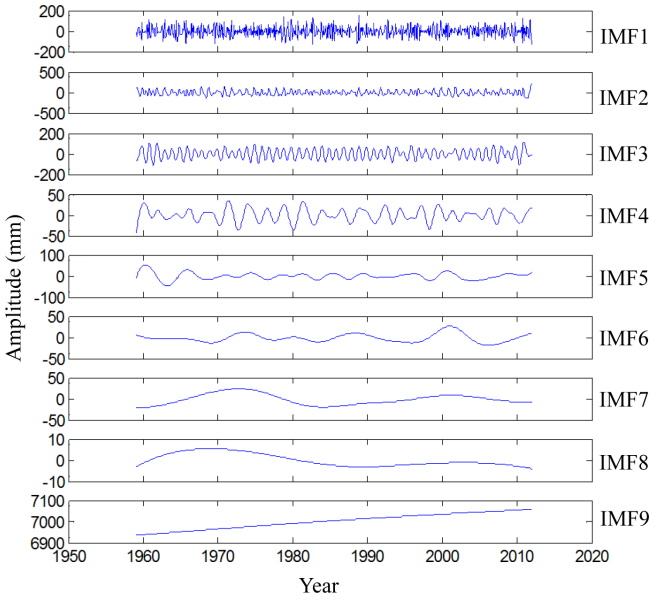

Fig. 2. IMFs obtained by decomposing Zhapo tide gauge records using EEMD.

level of 95%, suggesting that these six IMFs have statistical meaning. A linear trend of 1.6 mm/year can be observed from IMF 9, indicating that during the period of 1959–2011, the sea level around Zhapo rises at the rate of 1.6 mm/year, similar to rates found in other stations in the region [30] and similar to the global rate of 1.7 mm/year [31]. The results suggest that EEMD can extract the meaningful signals from the nonlinear and nonstationary time series, which would be appropriate for the study of sea level change.

Because of the complication and significance of sea level variability, many attempts have been devoted to it and several cycles (e.g., seasonal cycle) determined by different factors such as river flow and El Niño–Southern Oscillation (ENSO) have been found in the sea level time series [32]. In this decomposition, IMF 1 with mean period of 3 months represents the seasonal cycle of sea level change, and it may be controlled by local factors such as river flow [33]. IMF 2 and IMF 3, with mean period of 7 and 13 months, are supposed to be semi-annual and annual cycles, respectively. And these cycles are confirmed existing in most of sea level time series all over the world [34]. IMF 5 shows the similar cycle (49 months) with ENSO cycle which is almost 3–7 years [35]. Furthermore, while the end effects of IMF 5 have been removed [36], a negative correlation (R = –0.62) is observed between IMF 5 and the NINO 3.4 Sea Surface Temperature index. The result indicates that IMF 5 is related to the ENSO events. The mean period of IMF 6 (121 months) is consistent with solar magnetic activity cycle (11 years) [37]. A significant correlation (R = 0.82) is found between IMF 6 and the monthly series of mean northern hemisphere sunspot numbers, which was collected from Sunspot Index and Long-term Solar Observations. This high correlation suggesting that IMF 6 may reflect the response of sea level change to solar magnetic activity. The mean period of IMF 7 (220 months) is similar to the lunar nodal cycle (18.61 years). These are

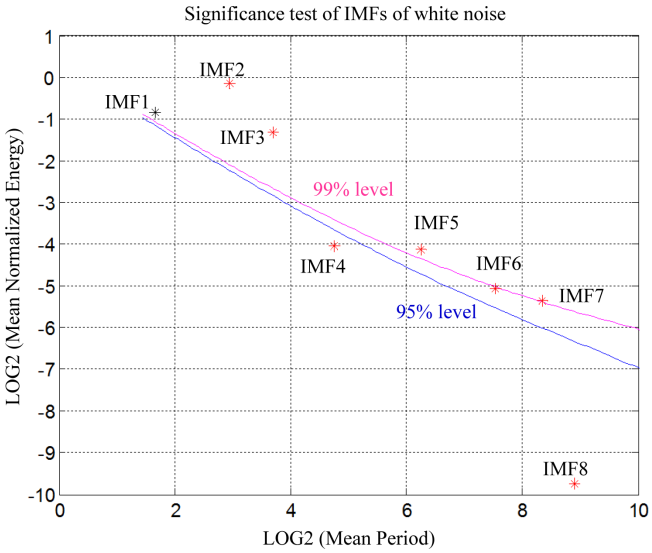

Fig. 3. IMF significance test of Zhapo tide gauge records with 99% (purple line) and 95% (blue line) confidence limit. The point (*) below the lines indicate that the hypothesis that the corresponding IMFs of the observations are not distinguishable from the corresponding IMFs of a random noise series cannot be rejected with the confidence levels (95% and 99%, respectively).

encouraging results indicating that the EEMD can extract the signals with physical meaning from the chaos series. Moreover, the variance contribution rate of each IMF shows that the first three IMFs explains most of the total variances, which are 30.71%, 42.88% and 20.05%, respectively. It suggests that the inter-annual, seasonal and annual cycles may be the dominant changes of the sea level in the study area, which is consistent with the study of Zheng [38] who reveals that the inter-annual variability would be the dominant characteristic of sea level in China.

3.2. Effects of neural network structure

The BP neural network structure is used to illustrate the performance for sea level modeling, which is optimized by setting the essential parameters such as the number of the hidden layers and the number of neurons in each layer, the learning rates (α), the momentum factor (η), the number of training iterations (epochs) and so on. Many studies have revealed that the typical BP neural network with one hidden layer can highly approximate any nonlinear function defined by sets of real number [39]. Thus, a BP neural network with three layers is adopted in this study for modeling the sea level prediction. The neurons of the hidden layer are used for extracting and restoring the rules from the samples, and the weights of them are critical to the reflecting function of the BP neural network. A testing BP neural network with α = 0.2, η = 0.9 and after 5,000 iterations is presented in Table 1 to illustrate the effect of the different number of the neurons. The results show that the prediction performance is improved when the neuron number increases until the number is over 6. Less neurons would result in absorbing information incompletely, while too much would extract the noise and lead to the over-fitting. Therefore, after many tests, the number of neurons was recommended to be 6.

The value of α affects the convergence of the BP neural network training process, and the proper value of momentum factor can avoid stopping the learning process at a local minimum instead of global minimum. Either low α or high η would fasten the convergence of the BP learning algorithm. After some preliminary tests, the learning rate and the momentum factor are listed in Table 2. Considering the different characteristics of the nine IMFs, the testing process is repeated and the parameter settings of the nine IMFs are shown in Table 2.

To evaluate the accuracy of the BP neural network, the comparison between the prediction and observation of IMFs 1–9 during 01/2007–12/2011 are shown in Fig. 4. All the

Table 1
Effect of the number of the hidden neurons

Time series	Number of hidden neurons	RMSE (mm)
Zhapo	1	98.793
	3	64.502
	5	42.814
	6	38.239
	7	44.787
	9	61.638
	11	67.326

predictions exhibit good performances. IMF 1 with the highest frequency signals exhibits a relatively poor performance, but the amplitudes and trends of the prediction are consistent with the observed value. IMFs 2–4 perform better than IMF 1, and as the signals go smoother, the prediction performances better. IMFs 8–9, the smoothest signals give the best performances in BP neural network prediction. These regular changing results indicate that BP neural network is suitable for the prediction of nonstationary and nonlinear time series, and the model will provide a higher level accuracy while the signal is smoother. By the way, when the prediction of long-term sea level change is carried, the high frequency in the signals such as seasonal cycle should be removed at first [40]. Therefore, the relatively poor performance of IMF 1 would make little effect on the prediction of the long-term sea level change.

Table 2
BP neural network structures of the nine IMFs for the sea level prediction

Time series	Number of hidden layers	Number of neurons	α	η	Epoch	RMSE (mm)
IMF1	1	6	0.01	0.9	5000	61.187
IMF2	1	6	0.04	0.9	5000	46.848
IMF3	1	6	0.1	0.7	5000	43.405
IMF4	1	6	0.02	0.8	5000	11.421
IMF5	1	6	0.1	0.8	5000	1.537
IMF6	1	6	0.01	0.8	5000	1.430
IMF7	1	6	0.01	0.9	5000	0.255
IMF8	1	6	0.1	0.7	5000	0.069
IMF9	1	6	0.1	0.7	5000	0.081

4. Discussions

The comparison between the predictions produced by the hybrid method and BP neural network directly is shown in Fig. 5. The high coincidence of the two prediction curves with the observation value curve indicates a good performance of the BP neural network for the sea level prediction. Nevertheless, more and larger deviations are found in the green curve when the two prediction curves are compared with the observed curve, such as in 10/2007, the value on green curve is significantly higher than that of observed data, while the EEMD-BP prediction is much closer to it. This phenomenon also appears in 10/2008 and 5/2010, where the green curve was clearly deviated from the red and blue curves. Fig. 4 shows that the red line is more approaching to the blue curve than the green curve does, which indicates that the hybrid method provides a better performance in sea level prediction than using the BP learning algorithm only. Moreover, larger

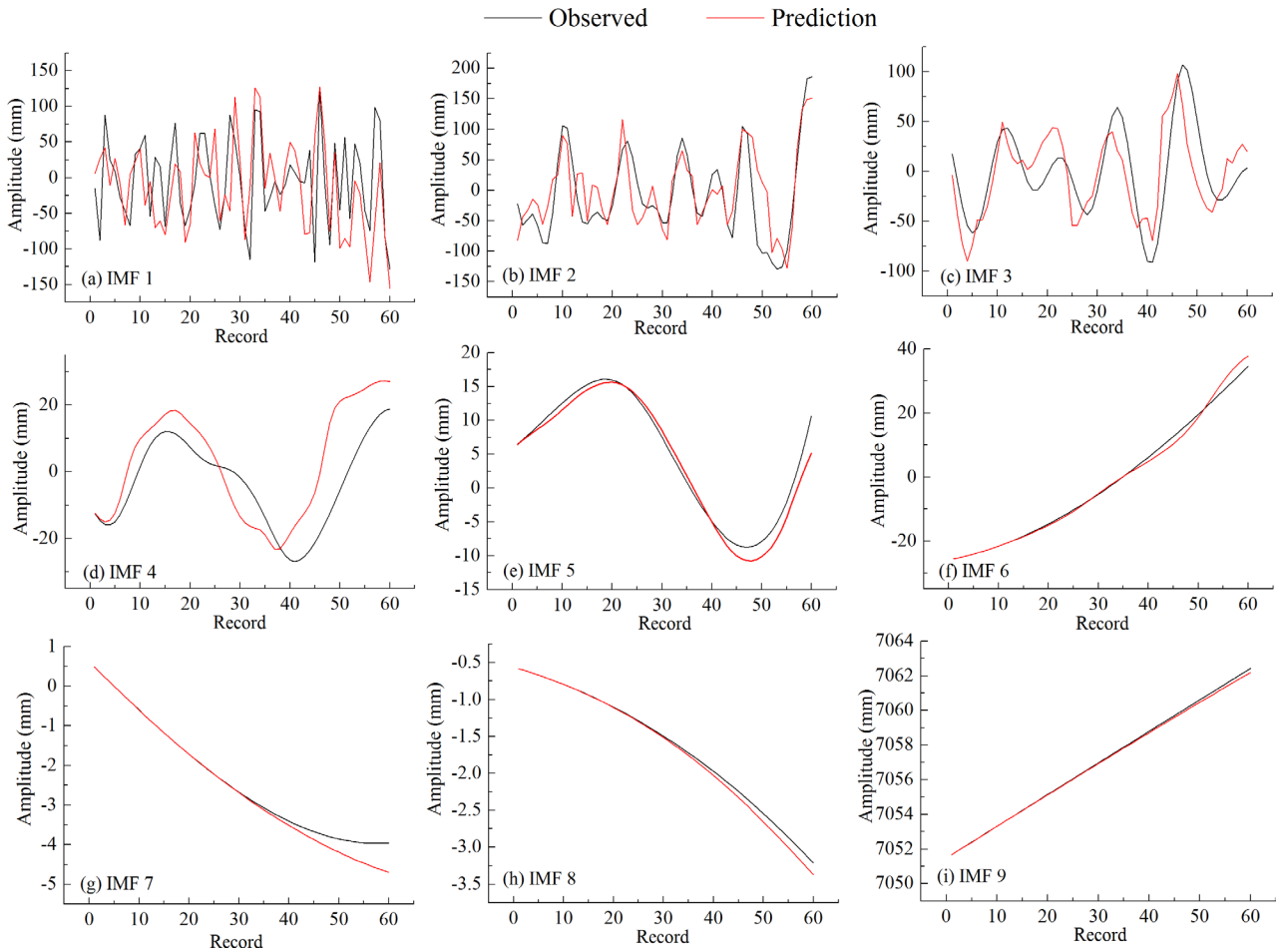

Fig. 4. Comparison between the prediction and samples of IMFs from EEMD.

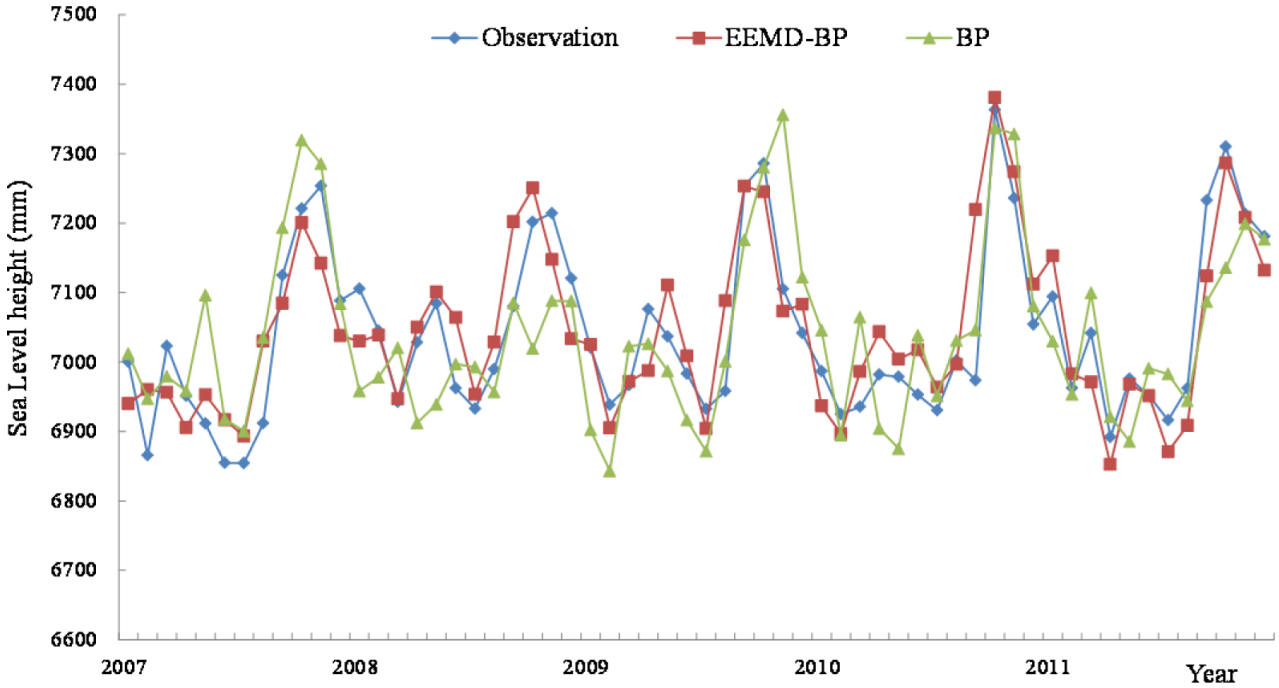

Fig. 5. Comparison between the predictions of the hybrid method and BP neural network (the blue line represents the observed data, the red line and green line represents the predictions from the hybrid method and BP neural network, respectively).

deviations of the BP neural network predictions are prone to appear in the extremes, for example, in 10/2007, 10/2008, 10/2011, which may suggest that the BP neural network has a relative poor ability in simulating extremes owing to the disorder and complex variability of the nonlinear original series. And the decomposition process has made an advantage for resolving this problem, as shown in Fig. 5.

The correlation coefficient (R) and the root square mean error (RMSE) are determined from the two predictions. High R and low RMSE between the predictions and the observation are the encouraging results indicating that the BP performs well in the sea level prediction. Compared with Cheng et al. [41] who carried out a prediction using tide gauge records and altimeter satellite data, and the minimum RMSE is 43.9 mm, the predictions in this study show a lower error level, would be applicable for sea level prediction (the higher RMSE produced by using the BP directly is 36.74 mm). Compared with using the BP method directly (with R = 0.76 and RMSE = 36.74 mm), the EEMD-BP hybrid method with higher R (R = 0.89) and lower RMSE (RMSE = 28.16 mm), shows a better performance. Lee [42] also used BP neural network for long-term tidal prediction, and the lowest normalized RMSE is 0.0844. The RMSE of the prediction produced by EEMD-BP is calculated accordingly, which is 0.0142, indicating that the hybrid method may improve the accuracy of the BP prediction.

5. Conclusions

Conventional methods developed for the sea level prediction are still considered insufficient due to the complexity of the nonstationary and nonlinear sea level change. In this study, a method combining the data analysis method EEMD and the prediction method BP neural network was proposed to improve the accuracy of sea level prediction. EEMD can extract significant information and wipe off the noise from sea level height time series, and is applicable for the sea level change analysis. The decomposition of Zhapo tide gauge records shows that the inter-annual and annual cycles are the dominant periods of sea level change in Guangdong, and the sea level has been rising at the rate of 1.6 mm/year during 1959–2011. With the advantages of not requiring the prior knowledge, BP neural network performs good in learning and predicting nonlinear and nonstationary time series by data driven. Preprocessing of the time series in the time and frequency allows defining the input of the BP neural network. The results show that the prediction accuracy has been improved when the input time series are decomposed to be smoother and more regular. The EEMD-BP hybrid method shows a higher accuracy (with R = 0.89 and RMSE = 28.16 mm) than using the BP neural network directly (with R = 0.76 and RMSE = 36.74 mm), and the hybrid method can be further applied to other regions for the sea level prediction. The results also illustrate that the pre-processing such as smoothing or decomposing is strongly recommended for the nonlinear time series prediction.

Acknowledgments

This study was conducted under the auspices of National Natural Science Foundation of China (41571041, 41601453), the Opening Fund of Key Laboratory of Poyang Lake Wetland and Watershed Research (Jiangxi Normal University), Ministry of Education (No. ZK2015001), Jiangxi Province Department of Education Science and technology research project (GJJ150306), and the Construction Service Program for Cultivating Unique Institution of the Chinese Academy of Sciences (TSYSJ04). The authors would like to specially thank the PSMSL for providing the tide gauge data, National

Climatic Data Center for providing NINO 3.4 index and SILSO for the sunspot numbers data. The authors are grateful to Xiangsheng Yi for assistance in the BP model establishment.

References

[1] S. Jevrejeva, J.C. Moore, A. Grinsted, Sea level projections to AD2500 with a new generation of climate change scenarios, Global Planet. Change, 80–81 (2012) 14–20.
[2] D.P. Chambers, C.A. Mehlhaff, T.J. Urban, R.S. Nerem, Analysis of interannual and low-frequency variability in global mean sea level from altimetry and tide gauges, Phys. Chem. Earth, 27 (2002) 1407–1411.
[3] J. Pycroft, L. Vergano, C. Hope, The economic impact of extreme sea-level rise: ice sheet vulnerability and the social cost of carbon dioxide, Global Environ. Change, 24 (2014) 99–107.
[4] C.L. Lopes, P.A. Silva, J.M. Dias, A. Rocha, A. Picado, S. Plecha, A.B. Fortunato, Local sea level change scenarios for the end of the 21st century and potential physical impacts in the lower Ria de Aveiro (Portugal), Cont. Shelf Res., 31 (2011) 1515–1526.
[5] A.B.A. Slangen, C.A. Katsman, R.S.W. van de Wal, L.L.A. Vermeersen, R.E.M. Riva, Towards regional projections of twenty-first century sea-level change based on IPCC SRES scenarios, Clim. Dyn., 38 (2012) 1191–1209.
[6] R.A. Bindschadler, S. Nowicki, A. Abe-Ouchi, A. Aschwanden, H. Choi, J. Fastook, G. Granzow, R. Greve, G. Gutowski, U. Herzfeld, C. Jackson, J. Johnson, C. Khroulev, A. Levermann, W.H. Lipscomb, M.A. Martin, M. Morlighem, B.R. Parizek, D. Pollard, S.F. Price, D.D. Ren, F. Saito, T. Sato, H. Seddik, H. Seroussi, K. Takahashi, R. Walker, W.L. Wang, Ice-sheet model sensitivities to environmental forcing and their use in projecting future sea level (the SeaRISE project), J. Glaciol., 59 (2013) 195–224.
[7] J.A. Church, D. Monselesan, J.M. Gregory, B. Marzeion, Evaluating the ability of process based models to project sea-level change, Environ. Res. Lett., 8 (2013) 014051.
[8] D. Felsenstein, M. Lichter, Social and economic vulnerability of coastal communities to sea-level rise and extreme flooding, Nat. Hazard., 71 (2014) 463–491.
[9] S. Rahmstorf, A semi-empirical approach to projecting future sea-level rise, Science, 315 (2007) 368–370.
[10] R.S. Nerem, B.D. Beckley, J.T. Fasullo, B.D. Hamlington, D. Masters, G.T. Mitchum, Climate-change-driven accelerated sea-level rise detected in the altimeter era, Proc. Natl. Acad. Sci. USA, 115 (2018) 2022–2025.
[11] Q.Y. Liu, M. Feng, D.X. Wang, ENSO-induced interannual variability in the southeastern South China Sea, J. Oceanogr., 67 (2011) 127–133.
[12] N.E. Huang, Z. Shen, S.R. Long, M.L.C. Wu, H.H. Shih, Q.N. Zheng, N.C. Yen, C.C. Tung, H.H. Liu, The empirical mode decomposition and the Hilbert spectrum for nonlinear and non-stationary time series analysis, Proc. Roy. Soc. A, 454 (1998) 903–995.
[13] L.C. Wu, C.C. Kao, T.W. Hsu, K.C. Jao, Y.F. Wang, Ensemble empirical mode decomposition on storm surge separation from sea level data, Coast Eng. J., 53 (2011) 223–243.
[14] Y.C. Cheng, T. Ezer, L.P. Atkinson, Q. Xu, Analysis of tidal amplitude changes using the EMD method, Cont. Shelf Res., 148 (2017) 44–52.
[15] Y.J. Xue, J.X. Cao, R.F. Tian, A comparative study on hydrocarbon detection using three EMD-based time-frequency analysis methods, J. Appl. Geophys., 89 (2013) 108–115.
[16] Z. Wu, N.E. Huang, Ensemble empirical mode decomposition: a noise-assisted data analysis method, Adv. Data Anal., 1 (2009) 1–41.
[17] R.H. Jones, Maximum likelihood fitting of ARMA models to time series with missing observations, Technometrics, 22 (1980) 389–395.
[18] V.V. Srinivas, B. Basu, D. Nagesh Kumar, S.K. Jain, Multi-site downscaling of maximum and minimum daily temperature using support vector machine, Int. J. Climatol., 34 (2014) 1538–1560.
[19] F.-M. Tseng, H.-C. Yu, G.-H. Tzeng, Applied hybrid grey model to forecast seasonal time series, Technol. Forecasting Social Change, 67 (2001) 291–302.
[20] A. Filippo, A.R. Torres, B. Kjerfve, A. Monat, Application of artificial neural network (ANN) to improve forecasting of sea level, Ocean Coastal Manage., 55 (2012) 101–110.
[21] H.C. Yuan, M.X. Tan, W.J. Wang, Selection of methods for predicting tidal levels with a typhoon surge effect, J. Coastal Res., 73 (2015) 337–341.
[22] S. Hallegatte, C. Green, R.J. Nicholls, J. Corfee-Morlot, Future flood losses in major coastal cities, Nat. Clim. Change, 3 (2013) 802–806.
[23] R.J. Nicholls, A. Cazenave, Sea-level rise and its impact on coastal zones, Science, 328 (2010) 1517–1520.
[24] L. He, G.S. Li, K. Li, Y.Q. Shu, Estimation of regional sea level change in the Pearl River Delta from tide gauge and satellite altimetry data, Estuarine Coastal Shelf Sci., 141 (2014) 69–77.
[25] B.Q. Huang, A. Kunoth, An optimization based empirical mode decomposition scheme, J. Comput. Appl. Math., 240 (2013) 174–183.
[26] Z.H. Wu, N.E. Huang, A study of the characteristics of white noise using the empirical mode decomposition method, Proc. Roy. Soc. A, 460 (2004) 1597–1611.
[27] D.E. Rumelhart, G.E. Hinton, R.J. Williams, Learning representations by back-propagating errors, Nature, 323 (1986) 533–536.
[28] J.A. Church, N.J. White, R. Coleman, K. Lambeck, J.X. Mitrovica, Estimates of the regional distribution of sea level rise over the 1950-2000 period, J. Clim., 17 (2004) 2609–2625.
[29] T. Lee, T.B.M.J. Ouarda, An EMD and PCA hybrid approach for separating noise from signal, and signal in climate change detection, Int. J. Climatol., 32 (2012) 624–634.
[30] T. Chen, Q. Yang, X. Xu, The characteristics of sea level change along the coast of Guangdong Province, Tropic Oceanol., 16 (1997) 95–100.
[31] J.A. Church, N.J. White, A 20th century acceleration in global sea-level rise, Geophys. Res. Lett., 33 (2006) 313–324.
[32] G.I. Roden, Low-frequency sea level oscillations along the Pacific Coast of North America, J. Geophys. Res., 71 (1966) 4755–4776.
[33] R.R. Torres, M.N. Tsimplis, Seasonal sea level cycle in the Caribbean Sea, J. Geophys. Res., 117 (2012) C07011.
[34] F.M. Calafat, D.P. Chambers, M.N. Tsimplis, Inter-annual to decadal sea-level variability in the coastal zones of the Norwegian and Siberian Seas: the role of atmospheric forcing, J. Geophys. Res., 118 (2013) 1287–1301.
[35] M. Marcos, A. Amores, Quantifying anthropogenic and natural contributions to thermosteric sea level rise, Geophys. Res. Lett., 41 (2014) 2502–2507.
[36] F.J. Wu, L.S. Qu, An improved method for restraining the end effect in empirical mode decomposition and its applications to the fault diagnosis of large rotating machinery, J. Sound Vib., 314 (2008) 586–602.
[37] G. Brasseur, P.C. Simon, Stratospheric chemical and thermal response to long-term variability in solar UV irradiance, J. Geophys. Res., 86 (1981) 7343–7362.
[38] W. Zheng, Distribution of annual rates of sea level and variation of long-period constituents in China, Mar. Sci. Bull., 18 (1999) 1–10.
[39] B. Pradhan, S. Lee, Regional landslide susceptibility analysis using back-propagation neural network model at Cameron Highland, Malaysia, Landslides, 7 (2010) 13–30.
[40] B.N. Asmar, P. Ergenzinger, Long-term prediction of the water level and salinity in the Dead Sea, Hydrol. Process., 16 (2002) 2819–2831.
[41] Y.C. Cheng, O.B. Andersen, P. Knudsen, Integrating non-tidal sea level data from altimetry and tide gauges for coastal sea level prediction, Adv. Space Res., 50 (2012) 1099–1106.
[42] T.L. Lee, Back-propagation neural network for long-term tidal predictions, Ocean Eng., 31 (2004) 225–238.